Available online at www.sciencedirect.com

ScienceDirect

Proceedings of the Combustion Institute 39 (2023) 1763–1772

Proceedings of the Combustion Institute

www.elsevier.com/locate/proci

A study of propagation of spherically expanding flames at low pressure using direct measurements and numerical simulations

Marie-Eve Clavel [a,b], Pierre Schleuniger [a], Yiqing Wang [c], Alexis Vandel [a], Vincent Modica [a], Zheng Chen [c], Bruno Renou [a,*]

[a] *INSA Rouen-Normandie, UNIROUEN, CNRS, CORIA, Normandie University, Rouen 76000, France*
[b] *Safran Aircraft Engines Villaroche, Moissy-Cramayel 77550, France*
[c] *SKLTCS, Department of Mechanics and Engineering Science, College of Engineering, Peking University, Beijing 100871, China*

Received 14 December 2021; accepted 15 July 2022
Available online 16 September 2022

Abstract

The outwardly propagating spherical flame (OPF) method is widely used to measure the laminar burning velocity (LBV). However, there are still numerous challenges to perform unambiguous measurements for extreme conditions, mainly for high and low (sub-atmospheric) pressures. In this work, the density weighted displacement speeds relative to burned ($\widetilde{S_{d,b}}$) and fresh gases ($\widetilde{S_{d,u}}$) are considered to report LBV for a large range of sub-atmospheric pressure (from 1 to 0.3 bar), equivalence ratio and fuels (methane and *n*-decane). These stretched flame speeds are obtained from experiments by using advanced optical diagnostics and the spherical flame propagation is simulated by the code A-SURF with different kinetic schemes to perform a direct comparison with the experimental results. It is shown that $\widetilde{S_{d,b}}$ is significantly affected by the pressure decrease and becomes strongly non-linear with flame stretch. This is explained by the finite flame thickness structure and qualitatively modeled by the finite thickness expression (FTE) model used for extrapolation at zero stretch. However, assumptions (equilibrium and static burned gases) made to report $\widetilde{S_{d,b}}$ are no longer valid and leads to strong under-prediction of LBV from extrapolation especially at low pressures. The shape of $\widetilde{S_{d,u}}$ is less impacted by the pressure decreases and a linear behavior with flame stretch is globally found even for strong sub-atmospheric conditions. However, the temperature of the fresh gas isotherm where $\widetilde{S_{d,u}}$ is extracted is not rigorously equal to the fresh gas's temperature, and a correction factor is required to get accurate LBV. Therefore, a direct comparison of $\widetilde{S_{d,u}}$ instead of extrapolated LBV between experimental and

* Corresponding author.
E-mail address: bruno.renou@insa-rouen.fr (B. Renou).

https://doi.org/10.1016/j.proci.2022.07.161

numerical data seems necessary to validate kinetic schemes at low pressures. A brief discussion is conducted on the validation of FFCM-1 and GRI3.0 for methane and Dryer mechanisms for *n*-decane at low pressures.

Keywords: Outwardly propagating flame; Laminar burning velocity; Low pressure; Methane; *N*-decane

1. Introduction

The laminar burning velocity (LBV) is a critical fuel/air mixture property which is essential for the validation of chemical kinetics and the modeling of turbulent combustion [1]. The Outwardly Propagating Flame (OPF) configuration is currently used by many research groups due to inherent facilities and advantages at ambient conditions. However, numerous challenges remain to perform unambiguous measurements for extreme conditions, mainly in terms of very high and low (sub-atmospheric) pressures. Recent developments at elevated pressures with the constant volume approach [2,3] overcome these difficulties and pave the way for experimental conditions relevant to engine and gas turbine conditions. For low pressure, the constant pressure method is required, but the classical method based on the extrapolation of flame propagation speed relative to burned gases may fail for at least two reasons as it was shown recently numerically [4]. This method is called the Indirect Method (IM) and briefly reminded below:

$$\widetilde{S_{d,b}} = \frac{\rho_b}{\rho_u}\left(\boldsymbol{S_f} - \boldsymbol{u_b}\right)\cdot \boldsymbol{n} \tag{1}$$

where ρ_b and ρ_u are the burned and fresh gas densities, respectively. S_f is the absolute flame speed deduced from the time derivative of the flame radius, dR/dt. $\boldsymbol{u_b}$ is the burned gas velocity and $\boldsymbol{n}$ the unit vector pointing towards the fresh gases. This equation is systematically simplified into,

$$\widetilde{S_{d,b}} \simeq \frac{\rho_b^{eq}}{\rho_u} S_f \tag{2}$$

where ρ_b^{eq} is the burned gas density at adiabatic thermodynamic and chemical equilibrium conditions. Note that the burned gases are assumed to be at rest ($u_b = 0$). For atmospheric and high-pressure conditions, these assumptions are valid and the IM method can be used unambiguously. For sub-atmospheric conditions, the burned gases don't reach chemical equilibrium and consequently, the density ratio ρ_b^{eq}/ρ_u approximation can no longer be used to report LBV (Eq. (2)). In addition, the finite-structure of stretched flame requires to modify classical extrapolation models in which the finite flame thickness must be included to account for a stronger non-linearity at lower pressure [5]. For sub-atmospheric conditions in confined combustion chamber, the heat release zone becomes much wider and the adiabatic flame temperature is not immediately reached in burned gases. Consequently, the burned gases are not at chemical equilibrium. At the same time, a negative inverted flow of burned gases is also observed [4]. A negative inverted flow of burned gases is also induced by chemical non-equilibrium and can not be neglected as usual.

Other experimental strategies are required to provide direct measurements of LBV without these assumptions. One of the solutions is to use the displacement speed relative to fresh gases, called the Direct Method (DM):

$$\widetilde{S_{d,u}} = \left(\frac{dR}{dt} - u_u\right) \tag{3}$$

An experimental methodology was developed by Varea et al. [6], Bradley et al. [7], improved recently by Clavel et al. [8] and validated by direct and blinded comparisons with DNS [8,9]. This method is however limited by the lack of a clear definition of the fresh gases iso-surface free from dilatation which make linear or non-linear classical extrapolations to zero-stretch difficult [10,11]. However, and despite a non-accurate definition of the fresh gas iso-surface, this approach overcomes the main difficulties related to the application of the classical method when radiation, non-equilibrium and non-static flow effects are non-negligible. For sub-atmospheric conditions, the benefits of the approach were shown numerically by using 1D simulations [4], but no experimental confirmation was done yet, up to now.

Though high-pressure LBV measurements have many practical applications for gas turbine and engine applications, sub-atmospheric data are also of importance for at least aircraft applications, especially when dealing with high-altitude relight. Furthermore, the development of optical diagnostics to characterize combustion kinetics, as well as the interpretation of data and their quantification, is much simpler in low-pressure flames, mainly because collision effects are less prevalent and the flame front becomes thicker as pressure decreases. It is worth noting also that pressure not only influences the frequency of molecular collision but also differentiates the relative efficiencies of two-body branching reactions versus three-body termination reactions [12].

A brief literature review shows that sub-atmospheric LBV measurements are very scarce in

the literature, mainly due to the inherent experimental difficulties. The first set of data have been obtained by Egolfopoulos et al. [12] for CH_4/air flames, for the Counter Flow Flame (CFF) configuration. This database provides a reference for kinetic scheme validation [13,14]. Low pressure (below 0.3 atm) LBV have been measured also with Heat Flux Burner (HFB) configuration for CH_4/air and CH_4/H_2/air mixtures. This database highlights a curvature of the pressure dependence in semi-logarithmic coordinates of LBV, as predicted by the kinetic scheme. More recently, low pressure LBV for CH_4/air mixtures have been obtained from OPF configurations using the IM method [15]. The authors pointed out the difficulty to get accurate data with this method due to the finite flame thickness issue in extrapolation models and the non-equilibrium state of burned gases.

In this work, we propose to consider the OPF configuration and to report, for the first time to our knowledge, stretched flame speeds for lean, stoichiometric and rich CH_4/air flames and stoichiometric *n*-decane/air flames at low pressures. This latter fuel is well known to be a good kerosene surrogate for LBV measurement [16]. At the same time, the flame propagation is simulated with A-SURF code for a direct comparison with the experiments in order to :

- Analyze the effect of low pressure on stretched flame speeds $\widetilde{S_{d,b}}$ and $\widetilde{S_{d,u}}$,
- Quantify experimentally and numerically the differences between the two methods (DM and IM) to report LBV, and the origins and the values of the bias induced by each of these methods,
- Provide a database for LBV at low pressures for methane/air and *n*-decane/air mixtures for kinetic scheme validations.

2. Experimental and numerical set-up

The experiments have been conducted in the spherical stainless steel combustion chamber (equivalent chamber inner-radius 8.243 cm) of the CORIA laboratory. The details of the facility and the optical diagnostics which have been used to report simultaneously the flame radius and the fresh gas velocity profiles ahead of the flame front can be found in Varea et al. [6], Clavel et al. [8], Varea et al. [17]. Effects of flow seeding density for PIV measurements have been evaluated and don't impact the stretched flame speeds and the extrapolated values, even for low pressure conditions. Methane/air mixtures are investigated for lean ($\phi = 0.8$), stoichiometric and rich ($\phi = 1.2$) conditions, with a pressure varying from 1 to 0.3 bar, at $T = 293$ K. The operating conditions and the accuracy of the flow-meters are similar to those presented in Clavel et al. [8]. For *n*-decane/air flames, the methodology presented in Varea et al. [17] is followed. *n*-decane is vaporized in a Controlled Evaporator Mixer, CEM (Bronkhorst) and injected into the vessel through heated lines. All gases are premixed in a tank before being injected into the combustion chamber. An electrical heating system regulates the chamber temperature and ensures uniformity of the temperature field. *n*-decane/air mixtures are investigated for stoichiometric conditions, with a pressure varying from 1 to 0.4 bar, at $T = 373$ K. Lower pressure conditions were not ignitable. Uncertainty quantification has been done according to the methodology presented in Clavel et al. [8]. It accounts first for the initial conditions which may be slightly different from one experiment to another and the intrinsic uncertainty of the sensors. Second, effect of flame variability induced by ignition (energy variation, spark shape) and uncertainties induced by image processing routines are accounted for by performing a statistical analysis with a number of flame recordings per condition $N \geq 10$. Once these uncertainties are evaluated, they are propagated when flame stretch, flame speeds and extrapolations are computed.

Spherical flame propagation is simulated using the code A-SURF [18]. A-SURF solves the one-dimensional, unsteady, compressible, conservation equations for a multi-component reactive flow in a spherical coordinate using the finite volume method. The details on governing equations, numerical schemes, and code validation can be found in Chen et al. [18]. The simulation domain reproduces the experimental apparatus described above in terms of equivalent flame radius and thermodynamical conditions. In order to maintain adequate resolution of the propagating flame, dynamically adaptive mesh is utilized in A-SURF with a finest grid size of 8 μm. It is noted that radiation heat losses are not accounted for here, considering the high flame speeds and the small flame radii which are investigated here. Simulations are performed for CH_4 flames with two kinetic schemes. First, the GRI-mech 3.0 kinetic scheme [13] is considered. It is composed of 53 species and 325 elementary reactions. This is a commonly used mechanism in the literature, but not recently updated and validated with low pressure LBV data for methane/air mixtures [12]. A more recent mechanism (FFCM-1) is also considered in this study. It is composed of 38 species and 291 elementary reactions [14] and it has been tested for low pressure LBV data for methane/air mixtures [12,19]. For *n*-decane/air flames, the Dryer mechanism composed of 121 species and 866 elementary reactions is used [20]. To our knowledge, no LBV validations against experimental data have been done at low pressures.

Finally, Cantera is used to report the LBV from 1D planar and stationary flames. The simulations are performed with the same kinetic schemes and operating conditions as those in A-SURF. The mixture-averaged diffusion model is considered.

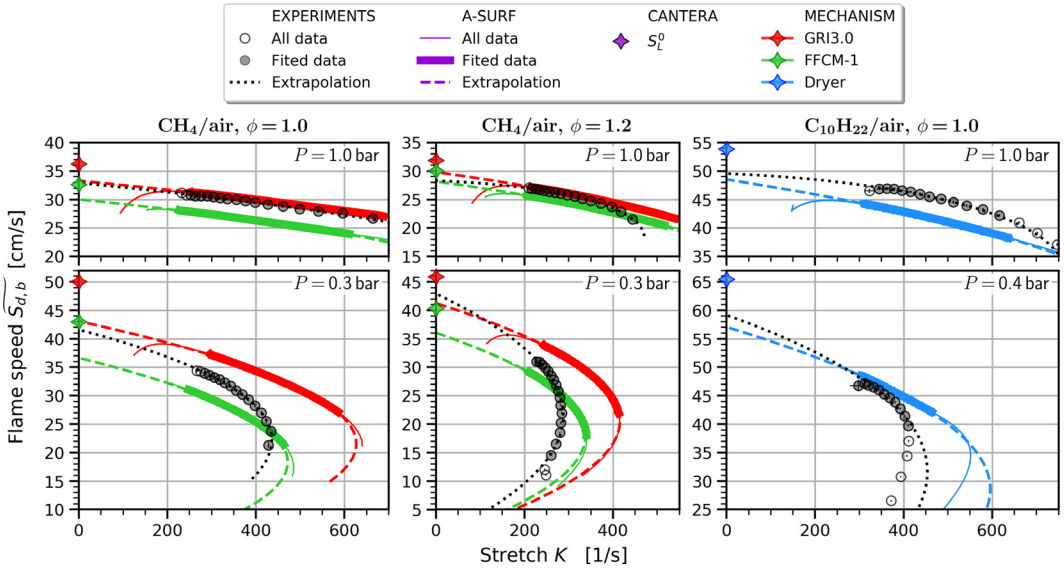

Fig. 1. Selected samples of stretched displacement speeds $\widetilde{S_{d,b}}$ for experiments and simulations, both for methane and *n*-decane air flames.

The computational domain is set to 5.0 cm. The minimum values of the gradient and curvature for the last iteration are set to 0.02.

3. Displacement speed relative to burned gases, $\widetilde{S_{d,b}}$

The displacement speed relative to burned gases $\widetilde{S_{d,b}}$ (Eq. (2)) is reported in Fig. 1 as a function of flame stretch K, with $K = (2/R)(dR/dt)$. For clarity, only two pressures are represented for methane and *n*-decane.

The lean methane/air flames behave similarly as the stoichiometric ones and are not represented here. However, these data are available in the Supplementary material. When the pressure decreases, the stretched flame speed becomes more sensitive to stretch, i.e. the slope increases in absolute value, and behaves less linearly. Similar observations are done both for experiments and simulations, whatever the kinetic schemes. This behavior can be explained by considering the original asymptotic solution for adiabatic outwardly propagating flames allowing for finite flame thickness [21]. In dimensional form, this solution becomes,

$$\left(\frac{S_f}{S_f^0}+\frac{2\delta_L^0}{R}\right)ln\left(\frac{S_f}{S_f^0}+\frac{2\delta_L^0}{R}\right)=-\frac{2(\mathcal{L}_b-\delta_L^0)}{R} \quad (4)$$

where S_f^0 is the extrapolated value of S_f and related to LBV by the density ratio such as $S_L^0 = (\rho_b^{eq}/\rho_u)S_f^0$, δ_L^0 is the flame thickness of the unstretched flame, and $\mathcal{L}_b$ is the Markstein length related to the burned gases. When assuming infinitely thin flame, the non-linear expression provided by Kelley and Law [22] can be easily recovered. This expression can then be simplified into the linear expression in case of low flame stretch and Lewis number close to unity. However, when the pressure decreases significantly, the flame thickness increases strongly making the assumption of infinitely thin flame no longer correct, as it was reported originally by Liang et al. [23] and was referred to as the finite thickness expression (FTE). Eq. (4) is generally expanded in terms of perturbation $\epsilon = 1/R$ for $\delta_L^0 \ll R$ to the third term,

$$\frac{S_f}{S_f^0}=1-2\mathcal{L}_b\epsilon-2(\mathcal{L}_b-\delta_L^0)^2\epsilon^2+\mathcal{O}(\epsilon^3) \quad (5)$$

Eq. (5) is used to extrapolate $\widetilde{S_{d,b}}$ at zero stretch, making the fitting procedure much more stable numerically than Eq. (4). In order to avoid ignition and confinement effects, a restricted range of flame radius for extrapolation has been set to [1, 1.9 cm] for experiments and to [0.8, 1.9 cm] for the simulations which seem to be less affected by ignition than experiments. This range is represented in bold lines and filled symbols in Fig. 1 and is in agreement with the usual recommendations [24]. For atmospheric conditions, stretched methane/air flame speeds are qualitatively very well predicted by the simulations with GRI3.0 for stoichiometric conditions, whereas the flame speeds from the simulations with FFCM-1 are smaller than those obtained with GRI3.0. The differences between the two kinetic schemes is however reduced for rich conditions which surround the experimental data. For stoichiometric *n*-decane/air flames, the simulations underpredict the experiments with a constant value close to 3 cm/s.

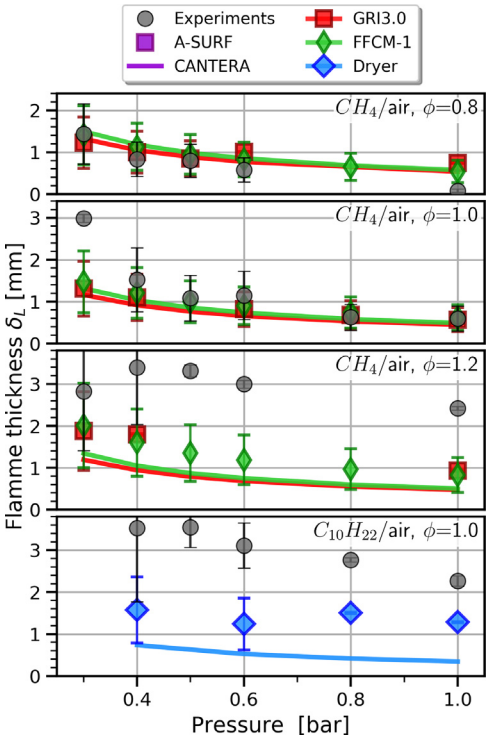

Fig. 2. Flame thickness, δ_L^0, deduced from the FTE model (Eq. (5)).

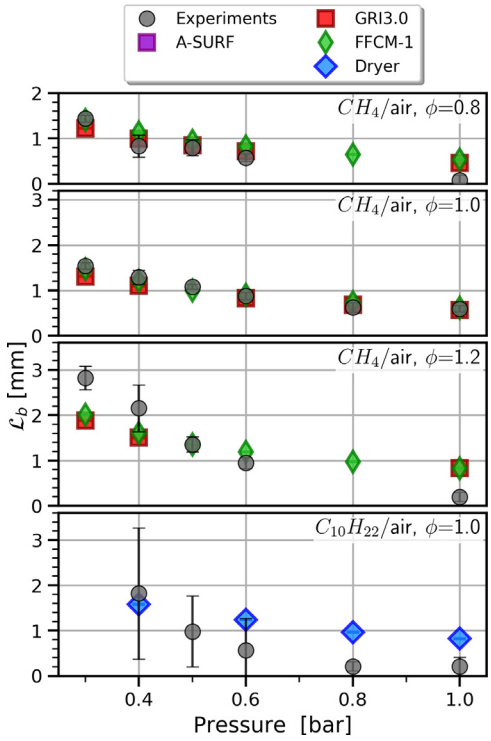

Fig. 3. Markstein Length, $\mathcal{L}_b$, deduced from the FTE model (Eq. (5)).

For sub-atmospheric conditions, the differences between the simulations with GRI3.0 and FFCM-1 are much more important and can reach a constant difference of 7 cm/s for stoichiometric conditions. The experimental data do not behave similarly with the simulations, in terms of slope and extrapolated values. As it stands, this qualitative comparison shows that these kinetic schemes are no longer able to predict the stretch evolution of $\widetilde{S_{d,b}}$ at very low pressure for such operating conditions. A more quantitative comparison between experiments and simulations can be done, by comparing the fitting parameters of Eq. (5), namely δ_L^0, $\mathcal{L}_b$ and S_L^0.

First, δ_L^0 is plotted in Fig. 2 and can be directly compared to δ_L^0 estimated from Cantera from the maximum temperature gradient, $\delta_L^0 = (T_b - T_u)/\nabla(T)_{\max}$. For stoichiometric methane/air flames, a globally good agreement between δ_L^0 (Cantera) and δ_L^0 from experiments and simulations can be found, even if the difference seems to be noticeable at very low pressure. The lower the pressure, the higher the flame thickness, and consequently, the $\widetilde{S_{d,b}}$ - K shape is more non-linear according to the FTE model. This observation underlines the quality of the fit, and the physical meaning of the FTE model for such conditions. However, significant differences are observed for rich methane/air flames with $\delta_L^0 \leq \delta_L^{ASURF} \leq \delta_L^{Exp.}$, and for n-decane/air flames as well. The origin of these differences is not understood and can not be overcome by changing significantly the radius range for extrapolation. The FTE model seems less appropriate and not able to predict the non-linear behavior.

Second, the Markstein length $\mathcal{L}_b$ is plotted in Fig. 3. Whatever the operating conditions, the pressure decrease leads to an increase of Markstein length. This is explained by the definition of the Markstein number $Ma_b = \mathcal{L}_b/\delta_L^0 = Le^{-1} - Z/2(Le^{-1} - 1)$ which is the Markstein length $\mathcal{L}_b$ normalized by δ_L^0. In this expression, Z is the Zeldovich number and Le the Lewis number. Ma_b does not depend on the pressure, and consequently $\mathcal{L}_b$ behaves in the same way as δ_L^0 with the pressure. A globally good agreement between experiments and simulations is observed, especially for lean and stoichiometric methane/air and n-decane/air mixtures, with very slight differences between GRI3.0 and FFCM-1 mechanisms. This is expected since $\mathcal{L}_b$ is a function of the overall activation energy, Lewis number and flame thickness. A significant change in the kinetic scheme doesn't affect $\mathcal{L}_b$ as it was shown by Xiouris et al. [3]. For rich condition, significant difference appears at low pressure, when $\widetilde{S_{d,b}}$ is strongly non-linear. Such a behavior on a re-

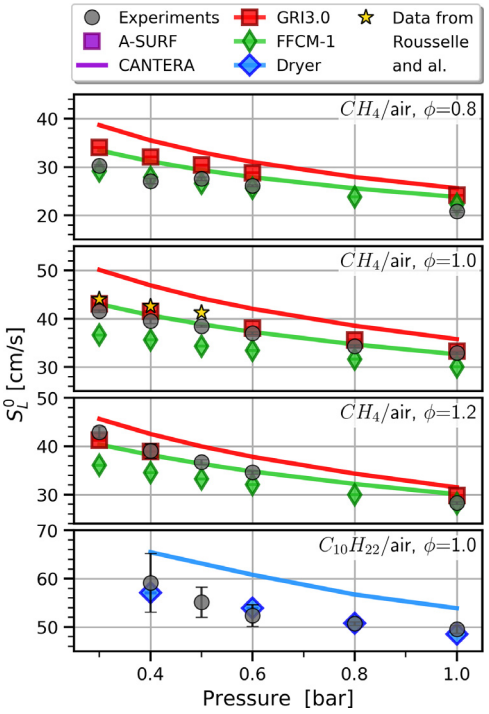

Fig. 4. Laminar burning velocity (LBV) deduced from extrapolation of $\widetilde{S_{d,b}}$ with the FTE model (Eq. (5)).

stricted range of flame radius seems difficult to be predicted by the FTE model.

Finally, the extrapolated flame speeds (LBV) from $\widetilde{S_{d,b}}$ are reported in Fig. 4. A deviation of extrapolated S_L^0 from simulations with those from predicted by Cantera is observed and it is about 2–3 cm/s for atmospheric conditions, and increases to 5–7 cm/s for P = 0.3 bar. These deviations were discussed in Clavel et al. [8] for atmospheric conditions, and explained by Faghih et al. [4] for very low pressure conditions considering the assumptions used in Eq. (2). This is a clear demonstration that LBV from $\widetilde{S_{d,b}}$ cannot be used as a target or validated cases for kinetic schemes at low pressures because of the issues coming from extrapolation models and assumptions. A similar conclusion was already suggested by Brequigny et al. [15] when studying experimental low pressure OPF for stoichiometric methane/air conditions.

4. Displacement speed relative to fresh gases, $\widetilde{S_{d,u}}$

The displacement speeds relative to fresh gases $\widetilde{S_{d,u}}$ are now considered using Eq. (3) and reported in Fig. 5 as a function of flame stretch. Still for clarity, only two pressures are considered. As for $\widetilde{S_{d,b}}$, data for lean methane stretched flame speeds $\widetilde{S_{d,u}}$ are presented in the Supplementary Material. $\widetilde{S_{d,u}}$ remains globally linear even at low pressure, except maybe for low pressure rich flames. This evolution is observed both experimentally and numerically. Regarding this linear behavior and the theoretical framework for stretched flame speeds $\widetilde{S_{d,u}}$ [11], a linear extrapolation model for all the operating conditions has been selected :

$$\widetilde{S_{d,u}} = S_L^0 - \mathcal{L}_u K \tag{6}$$

Since the flame surface isotherm where $\widetilde{S_{d,u}}$ is defined is independent of the flame structure (and consequently of flame thickness), the finite flame thickness is not introduced in the extrapolation model. $\widetilde{S_{d,u}}$ from A-SURF show a very large range of linear behavior (much more than for $\widetilde{S_{d,b}}$). The linear fit is well suited for extrapolation at zero stretch, even if this linear range is however reduced for rich CH_4/air, and stoichiometic *n*-decane/air flames at low pressures. Indeed, a restricted range of flame radius for extrapolation has been set to $[R_{\min}, 2.2\ \text{cm}]$ both for experiments and simulations, with $R_{\min}$ increasing from 0.7 cm for atmospheric pressure to 1.5 cm for the lowest pressure conditions. This is also true for experiments, except maybe for rich CH_4/air flames at low pressure, where a larger combustion chamber might be necessary. As a preliminary conclusion, $\widetilde{S_{d,u}}$ seems easier to be extrapolated at zero stretch than $\widetilde{S_{d,b}}$ since $\widetilde{S_{d,u}}$ is less sensitive to flow confinement and presents a linear behavior on a large range of flame radius. It would make the extrapolated data from $\widetilde{S_{d,u}}$ at low pressure more accurate and less affected by the range of flame radius.

The Markstein lengths $\mathcal{L}_u$ from linear extrapolations are reported in Fig. 6. $\mathcal{L}_u$ from experiments and simulations have globally the same slopes ($\mathcal{L}_u$ is similar) for lean and stoichiometric methane/air flames, with no influence of kinetic scheme for methane. However, due to the scatter of the experimental data, the fit seems more difficult to perform, and the uncertainty on $\mathcal{L}_u$ is also more significant than $\mathcal{L}_b$. An increase of $\mathcal{L}_u$ is observed when the pressure decreases. This is also expected since Ma_u is not pressure dependent. Extrapolated flame speeds from $\widetilde{S_{d,u}}$ are reported in Fig. 7. In a general manner, LBV from $\widetilde{S_{d,u}}$ is much higher than that from $\widetilde{S_{d,b}}$ as expected in Faghih et al. [4]. For stoichiometric methane/air flames, a perfect agreement between experimental LBV and Cantera with GRI3.0 is observed whatever the pressure. For rich methane/air flames, the agreement with Cantera GRI3.0 is weak, and the condition of 0.3 bar is not achievable experimentally due to the very limited range of linear behavior. For *n*-decane/air flames, experimental LBV are similar to those predicted by the Dryer mechanism, with a maximum absolute difference of 2 cm/s at 0.4 bar.

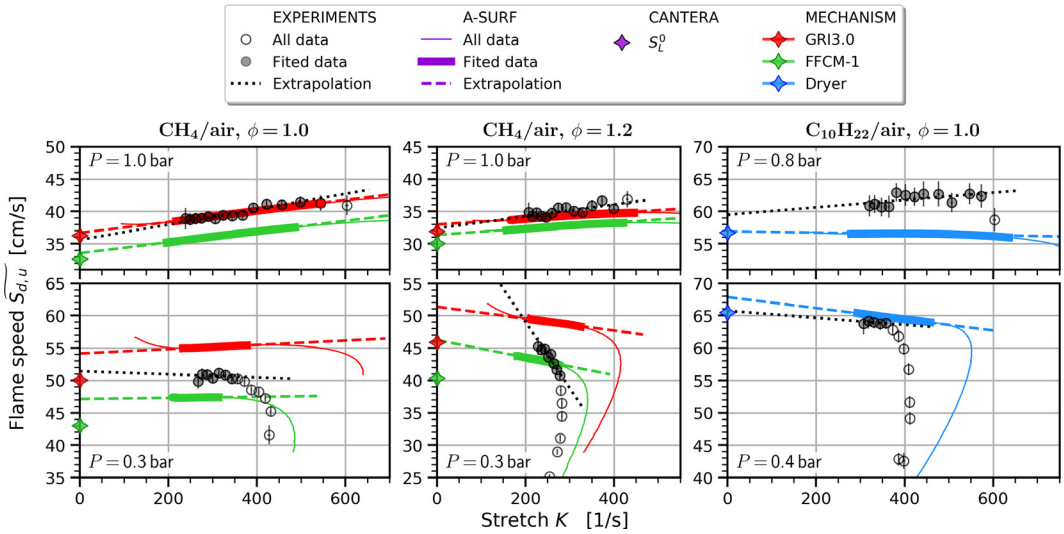

Fig. 5. Selected samples of stretched displacement speeds $\widetilde{S_{d,u}}$ for experiments and simulations, both for methane and *n*-decane air flames.

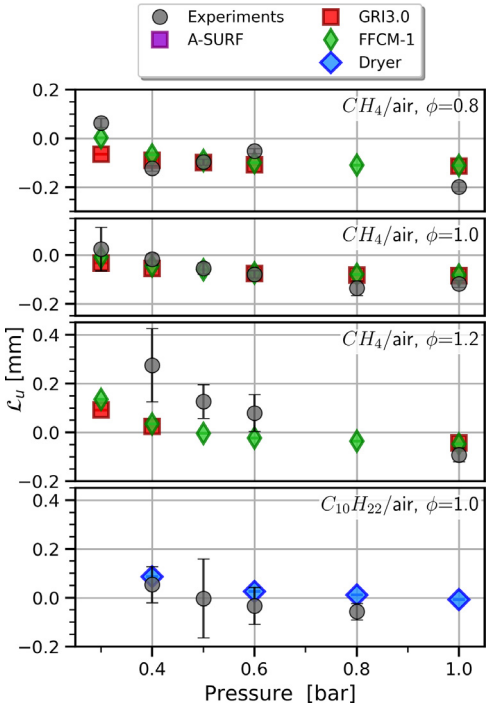

Fig. 6. Markstein Length, $\mathcal{L}_u$, deduced from the linear extrapolation of $\widetilde{S_{d,u}}$ to zero stretch using Eq. (6).

LBV from A-SURF behave similarly as experiments but do not agree exactly with Cantera values, especially at low pressures, where the difference is significant and on the order of 3 to 5 cm/s at 0.3 bar for methane/air flames whatever the kinetic scheme. This difference is however lower for *n*-decane/air flame even still visible. This behavior is unexpected regarding the previous work of Faghih et al. [4] and must be discussed. The experimental method to report LBV from $\widetilde{S_{d,u}}$ is based on Eq. (3) and implicitly assumes that the maximum of fresh gases velocity peaks at $T = T_u$. However, according to the present simulations and previous results in Jayachandran et al. [10], the temperature at the location of maximum velocity is slightly higher than T_u and decreases with stretch. Consequently, Eq. (6) should be corrected into :

$$\widetilde{S_{d,u}*} = \frac{\rho*}{\rho_u}\left(\frac{dR}{dt} - u_u\right) \tag{7}$$

where $\rho*$ is the flow density at which the fresh gas velocity is maximum. In the previous experimental works [6–8], this density ratio was assumed to be equal to unity. Though this assumption seems to be correct for atmospheric conditions, the results presented in Fig. 5 suggest that this assumption fails at lower pressure. From the simulations, we plotted this correction factor in Fig. 8 for methane and *n*-decane/air flames. In Fig. 8, the bold lines represent the correction factor values with the range of flame radius (or stretch) used for extrapolation. As expected, this correction factor is close to unity for atmospheric conditions and decreases significantly at lower pressure to reach 0.85 for the leanest conditions. Consequently, if Eq. (3) can be used for atmospheric conditions to report accurate date on LBV, the use of Eq. (7) is required for lower pressures. Accounting for this correction factor, the numerical values of $\widetilde{S_{d,u}*}$ are computed and extrapolated at zero stretch using Eq. (6) for the same range of flame radius as previously. These corresponding

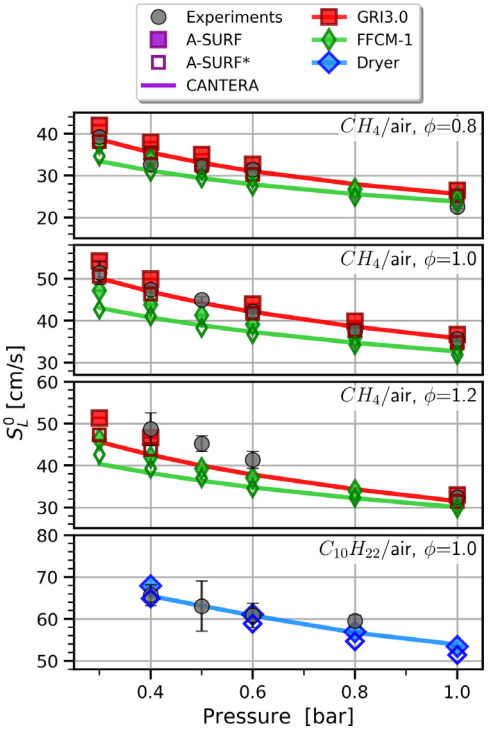

Fig. 7. Laminar burning velocity (LBV) deduced from extrapolation of $\widetilde{S_{d,u}}$ with linear model. The empty symbols corresponds to the LBV obtained from $\widetilde{S_{d,u}}*$ using Eq. (7).

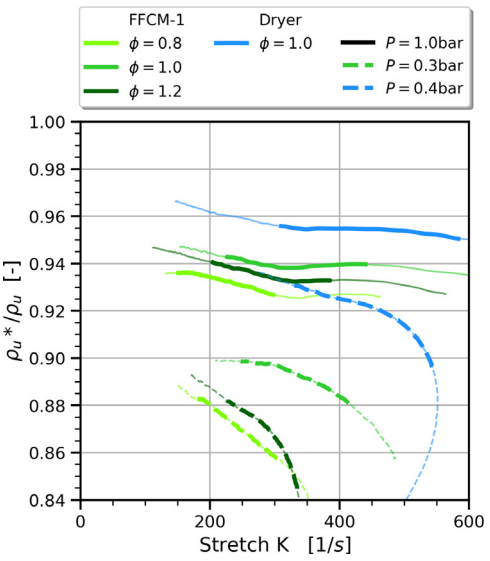

Fig. 8. Correction factor $\rho*/\rho_u$ for methane/air flames from the FFCM-1 mechanism. Very similar results are obtained with the GRI3.0 mechanism. This correction factor is also reported for *n*-decane/air flames.

LBV are reported in Fig. 7, with the empty symbols. A very good agreement can be now observed with LBV from Cantera and LBV from linear extrapolation of $\widetilde{S_{d,u}}$ from A-SURF using the same kinetic scheme.

5. Conclusions

Very few data for laminar burning velocity (LBV) at sub-atmospheric conditions are available in the literature and the kinetic schemes are generally not well validated or tested at low pressure conditions. In this work, LBV measurements at sub-atmospheric conditions have been conducted experimentally and numerically on methane/air and *n*-decane/air mixtures for several equivalence ratios in the OPF configuration. *n*-decane is known to be a relevant surrogate for kerosene when LBV is considered, and this work provides new measurements in conditions of high-altitude relight represented by low-pressure, by considering advanced measurements and simulations. The simulations have been done with two different kinetic schemes (namely GRI3.0 and FFCM-1) for methane/air and the Dryer mechanism is considered for *n*-decane/air flame. The main conclusions are three-folds. First, the flame displacement speed $\widetilde{S_{d,b}}$ is significantly impacted by the pressure decrease and becomes strongly non-linear with flame stretch. This is explained by the finite flame thickness structure and qualitatively well modeled by the FTE model used for extrapolation at zero stretch. At low pressures, assumption of static burned gases and chemical equilibrium usually made to report $\widetilde{S_{d,b}}$ are no longer valid and leads to a significant under estimation of $\widetilde{S_{d,b}}$. Consequently, the FTE model which also assumes static flow of burned gases is less prone to predict the $\widetilde{S_{d,b}}$ behavior as the flame propagates. In addition, due to the finite size of the combustion chamber and the very high sensitivity of range of flame radius used for extrapolation, this extrapolation at zero stretch may not be accurate. Second, the flame displacement speed $\widetilde{S_{d,u}}$ is less impacted by the pressure decreases and a linear behavior with stretch is globally found even for strong sub-atmospheric conditions, even if the range of linear behavior is reduced at low pressure. The finite flame thickness phenomenon doesn't affect the extrapolation methodology regarding the reference flame surface to report $\widetilde{S_{d,u}}$. Consequently, it makes the extrapolation easier in comparison with $\widetilde{S_{d,b}}$. However, the isotherm $T*$ where $\widetilde{S_{d,u}}$ is extracted is not exactly equal to T_u and a correction factor $\rho*/\rho_u$ is required. This correction factor is close to one at atmospheric conditions and decreases significantly at low pressure, leading to an overestimation of $\widetilde{S_{d,u}}$ if Eq. (3) is used, and consequently to the reported LBV values. Therefore, a direct comparison of $\widetilde{S_{d,u}}$ instead of LBV between experimental

and numerical data seems necessary to provide kinetic scheme validation as it was suggested initially by Jayachandran et al. [10]. This is particularly true when low pressure data are considered.Third, a direct comparison of $\widetilde{S_{d,u}}$ between experiments and simulations can be made considering the two conclusions above for kinetic scheme validations. For lean methane/air flames, FFCM-1 mechanism is in good agreement with the experiments for the range of pressure 0.3 to 1.0 bar. For stoichiometric conditions, GRI3.0 seems closer to experiments than FFCM-1. A significant departure between experiments and simulations is observed for rich flames which still under-predict $\widetilde{S_{d,u}}$. Finally, the Dryer mechanism seems well validated for the stoichiometric conditions over the range of pressure 0.4 to 1.0 bar.

Declaration of Competing Interest

The authors declare that they have no known competing financial interests or personal relationships that could have appeared to influence the work reported in this paper.

Acknowledgments

Financial supports from the French National Research Agency under the project RAFBIOALG (ANR-18-CE43-0009) and National Natural Science Foundation of China (No. 52176096) are gratefully acknowledged.

Supplementary material

Supplementary material associated with this article can be found, in the online version, at 10.1016/j.proci.2022.07.161.

References

[1] F.N. Egolfopoulos, N. Hansen, Y. Ju, K. Kohse-Hŋinghaus, C.K. Law, F. Qi, Advances and challenges in laminar flame experiments and implications for combustion chemistry, Prog. Energy Combust. Sci. 43 (0) (2014) 36–67.

[2] F. Halter, Z. Chen, G. Dayma, C. Bariki, Y. Wang, P. Dagaut, C. Chauveau, Development of an optically accessible apparatus to characterize the evolution of spherically expanding flames under constant volume conditions, Combust. Flame 212 (2020) 165–176.

[3] C. Xiouris, T. Ye, J. Jayachandran, F.N. Egolfopoulos, Laminar flame speeds under engine-relevant conditions: uncertainty quantification and minimization in spherically expanding flame experiments, Combust. Flame 163 (2016) 270–283.

[4] M. Faghih, Z. Chen, J. Huo, Z. Ren, C.K. Law, On the determination of laminar flame speed from low–pressure and super-adiabatic propagating spherical flames, Proc. Combust. Inst. 37 (2) (2019) 1505–1512.

[5] T. Shu, Y. Xue, W. Liang, Z. Ren, Extrapolations of laminar flame speeds from expanding spherical flames based on the finite-structure stretched flames, Combust. Flame 226 (2021) 445–454.

[6] E. Varea, V. Modica, A. Vandel, B. Renou, Measurement of laminar burning velocity and Markstein length relative to fresh gases using a new postprocessing procedure: application to laminar spherical flames for methane, ethanol and isooctane/air mixtures, Combust. Flame 159 (2) (2012) 577–590.

[7] D. Bradley, M. Lawes, M.E. Morsy, Flame speed and particle image velocimetry measurements of laminar burning velocities and Markstein numbers of some hydrocarbons, Fuel 243 (2019) 423–432.

[8] M.E. Clavel, A. Vandel, V. Modica, Z. Chen, E. Varea, V. Moureau, B. Renou, Determination of spatially averaged consumption speed from spherical expanding flame: a new experimental methodology, Combust. Flame 235 (2022) 111720.

[9] J. Jayachandran, A. Lefebvre, R. Zhao, F. Halter, E. Varea, B. Renou, F.N. Egolfopoulos, A study of propagation of spherically expanding and counter-flow laminar flames using direct measurements and numerical simulations, Proc. Combust. Inst. 35 (1) (2015) 695–702.

[10] J. Jayachandran, R. Zhao, F.N. Egolfopoulos, Determination of laminar flame speeds using stagnation and spherically expanding flames: molecular transport and radiation effects, Combust. Flame 161 (9) (2014) 2305–2316.

[11] G.K. Giannakopoulos, A. Gatzoulis, C.E. Frouzakis, M. Matalon, A.G. Tomboulides, Consistent definitions of æflame displacement speedg and æMarkstein lengthg for premixed flame propagation, Combust. Flame 162 (4) (2015) 1249–1264.

[12] F.N. Egolfopoulos, P. Cho, C.K. Law, Laminar flame speeds of methane-air mixtures under reduced and elevated pressures, Combust. Flame 76 (3) (1989) 375–391.

[13] G.P. Smith, D.M. Golden, M. Frenklach, N.W. Moriarty, B. Eiteneer, M. Goldenberg, C.T. Bowman, R.K. Hanson, S. Song, W.C. Gardiner, V.V. Lissianski, Z. Qin, http://www.me.berkeley.edu/grimech/, 1999.

[14] G. Smith, Y. Tao, H. Wang, Foundational fuel chemistry model version 1.0 (FFCM-1), http://nanoenergy.stanford.edu/ffcm1, 2016.

[15] P. Brequigny, H. Uesaka, Z. Sliti, D. Segawa, F. Foucher, G. Dayma, C. Mounaóm-Rousselle, Uncertainty in measuring laminar burning velocity from expanding methane-air flames at low pressures, 11th Mediterranean Combustion Symposium, Tenerife, Spain, 2019.

[16] Y. Wu, V. Modica, X. Yu, F. Grisch, Experimental investigation of laminar flame speed measurement for kerosene fuels: jet A-1, surrogate fuel, and its pure components, Energy Fuels 32 (2) (2018) 2332–2343.

[17] E. Varea, V. Modica, B. Renou, A.M. Boukhalfa, Pressure effects on laminar burning velocities and Markstein lengths for isooctane-ethanol-air mixtures, Proc. Combust. Inst. 34 (1) (2013) 735–744.

[18] Z. Chen, M.P. Burke, Y. Ju, Effects of Lewis number and ignition energy on the determination of laminar flame speed using propagating spherical flames, Proc. Combust. Inst. 32 (1) (2009) 1253–1260.

[19] M.I. Hassan, K.T. Aung, G.M. Faeth, Measured and predicted properties of laminar premixed methane/air flames at various pressures, Combust. Flame 115 (4) (1998) 539–550.
[20] M. Chaos, A. Kazakov, Z. Zhao, F.L. Dryer, A high--temperature chemical kinetic model for primary reference fuels, Int. J. Chem. Kinet. 39 (7) (2007) 399–414.
[21] M.L. Frankel, G.I. Sivashinsky, On effects due to thermal expansion and Lewis number in spherical flame propagation, Combust. Sci. Technol. 31 (3–4) (1983) 131–138.
[22] A.P. Kelley, C.K. Law, Nonlinear effects in the extraction of laminar flame speeds from expanding spherical flames, Combust. Flame 156 (9) (2009) 1844–1851.
[23] W. Liang, F. Wu, C.K. Law, Extrapolation of laminar flame speeds from stretched flames: role of finite flame thickness, Proc. Combust. Inst. 36 (1) (2017) 1137–1143.
[24] Z. Chen, On the accuracy of laminar flame speeds measured from outwardly propagating spherical flames: methane/air at normal temperature and pressure, Combust. Flame 162 (6) (2015) 2442–2453.